Processing and Application of Ceramics 11 [1] (2017) 21–26
BY-NC-ND
DOI: 10.2298/PAC1701021B

Investigation of structural transition in molybdates $CuMo_{1-x}W_xO_4$ prepared by polymeric precursor method

Mohamed Benchikhi[1,2,*], Rachida El Ouatib[1], Sophie Guillemet-Fritsch[2], Lahcen Er-Rakho[1], Bernard Durand[2]

[1]*Laboratoire de Physico-Chimie des Matériaux Inorganiques, Université Hassan II Casablanca, Morocco*
[2]*CNRS, Institut Carnot CIRIMAT, UMR CNRS-UPS-INP 5085, Université Paul-Sabatier, 118 route de Narbonne, 31062 Toulouse Cedex 9, France*

Received 23 August 2016; Received in revised form 5 December 2016; Accepted 2 February 2017

Abstract

Solid solutions ($CuMo_{1-x}W_xO_4$ where $0 \leq x \leq 0.12$) were synthesized by using a polymeric precursor method. The crystallization process of the polymeric precursors was investigated using TG-DTA, FTIR and XRD techniques. Crystallization of the $CuMo_{1-x}W_xO_4$ powders was detected at 300 °C, and entirely completed at 420 °C. XRD patterns revealed that the polymorphic variety was dependent upon the tungsten content. For $x \leq 0.075$, the solid solutions were isostructural to α-$CuMoO_4$ whereas, for $0.075 < x \leq 0.12$, they were isostructural to γ-$CuMoO_4$. The obtained homogeneous powders are constituted of relatively spherical grains with sizes in the range 0.5–2.0 μm. The phase transition of the as-synthesized $CuMo_{1-x}W_xO_4$ powders was investigated by X-ray diffraction at elevated temperature and dilatometry. The temperature of the structural transition $\gamma \rightarrow \alpha$ during heating was dependent upon the tungsten content.

Keywords: *thermochromism, sol-gel processes, thermal analysis, structural characterization*

I. Introduction

Because of their potential applications as temperature indicator, an intensive research on thermo-chromic materials was carried out [1–3]. Most of them are of organic type and their use is limited to applications at low temperature because of their low thermal stability. The thermo-chromic oxides are of special interest because of their high stability at high temperatures. Several mechanisms explain the change of their colour with temperature: dilatation and reduction of the ligand field on a chromophoric cation (e.g. in chromium doped alumina) [4], reduction of the band gap in semiconductors [5], or phase transition (e.g. in molybdates $AMoO_4$, where A is a 3d-transitional metal) [3,6,7]. The molybdate $CuMoO_4$ particularly exhibits a reversible phase transition α (green) $\rightarrow$ γ (brown-red) [1,3]. In the polymorph α-$CuMoO_4$, stable at high temperature and low pressure, the Cu^{2+} ions are located both in octahedral (CuO_6) and in pyramidal (CuO_5) sites. The Mo^{6+} cations are in tetrahedral environment (MoO_4) [3,8]. In the polymorph γ-$CuMoO_4$, stable at low temperature and high pressure, both metallic cations are in octahedral environment [3,8]. From standard conditions of temperature and pressure, the $\alpha \rightarrow \gamma$ transition occurs either by increase of pressure above 2.5 kbar or by cooling below 200 K [3]. Recently it has been shown that, in tungsten doped copper molybdate $CuMo_{1-x}W_xO_4$ ($x \leq 0.12$), the transition temperature and pressure are dependent upon the tungsten content [1]. Numerous authors have studied the optical, electrical, magnetic, and catalytic properties of $CuMoO_4$ [2,8–11].

The most general method to prepare molybdate powders involves solid state reaction of mixed parent oxides [8], which needs high temperature to overcome the energy barrier [12]. The powders obtained by this method are composed of large particles with an inhomogeneous composition. The inhomogeneous structure is formed because MoO_3 has tendency to volatilize at high temperatures [13]. For these reasons, various chemical methods have been investigated to prepare molybdates powders, such as co-precipitation method [1], polyol process [9], pyrolysis technique [14], electrochemical route [15]

* Corresponding author: tel: +212 660 793 843,
fax: +212 522 230 674, e-mail: *Benchikhi_mohamed@yahoo.fr*

and recently the citrate complex method [16,17]. This latter, allowing the control of the composition, the grain size and the homogeneity of powders [16–18], was chosen for the preparation of tungsten doped copper molybdate.

Solid solutions $CuMo_{1-x}W_xO_4$ were synthesized within the domain of solubility of tungsten in $CuMoO_4$ ($0 \leq x \leq 0.12$) and the phase transformation $\gamma \rightarrow \alpha$ was studied by X-ray diffraction and dilatometry.

II. Experimental

The solid solutions $CuMo_{1-x}W_xO_4$ were synthesized by the polymeric precursor method using the appropriate amounts of copper nitrate $Cu(NO_3)_2 \times 3\,H_2O$ (Acros organics, 99.9%), ammonium molybdate $(NH_4)_6Mo_7O_{24} \times 3\,H_2O$ (Sigma Aldrich, 99.8%), ammonium tungstate $(NH_4)_{10}W_{12}O_{41} \times 5\,H_2O$ (Acros organics, 99.0%) and citric acid (Acros organics, 99.9%). The synthesis procedure was similar to that used for the preparation of undoped α-$CuMoO_4$ [16]. The stoichiometric amounts of metal salts were dissolved separately in deionized water under magnetic stirring at room temperature. The obtained solutions were mixed together in order to obtain final molar ratio Cu : Mo : W = 1 : 1 − x : x (with x = 0.025, 0.05, 0.075, 0.100, 0,120). A citric acid (CA) solution was added to the mixture in a proportion such that CA/cation = 3. The solution was heated under magnetic stirring at 80–100 °C until the formation of a viscous liquid. The obtained gels were dried at 120 °C for 24 h and then pre-calcined at 300 °C for 12 h.

The crystallization process of the polymeric precursors was evaluated by thermogravimetry-differential thermal analysis (SETERAM TG-DTA 92) and infrared spectroscopy (FTIR, Perkin Elmer 1760). The crystalline structure was investigated by X-ray diffraction (Brucker AXSD4, $\lambda_{CuK\alpha}$ = 0.154056 nm, operating voltage 40 kV and current 40 mA) with a 0.02° step scan and 3.6 s/step. The microstructure and chemical composition of samples were analysed using scanning electron microscopy (SEM, JEOL JSM 6400 provided with energy dispersion X-EDS). The phase transition was investigated by X-ray diffraction (Brucker ASXD8 fitted with a high temperature chamber of MRI Radiation type) and dilatometry under air flux at a temperature rate of 2.5 °C/min (Setsys Evolution TMA Setaram).

III. Results and discussion

3.1. Structural characterization

Figure 1 shows the TG-DTA curves for the $CuMo_{0.9}W_{0.1}O_4$ gel dried at 120 °C. Considerable weight loss can be seen in the TG curve with temperature increase up to 420 °C. For temperature higher than 420 °C, there is no weight loss in the TG curve, confirming that combustion of all organic matter occurs below this temperature. The DTA curve indicates that there are

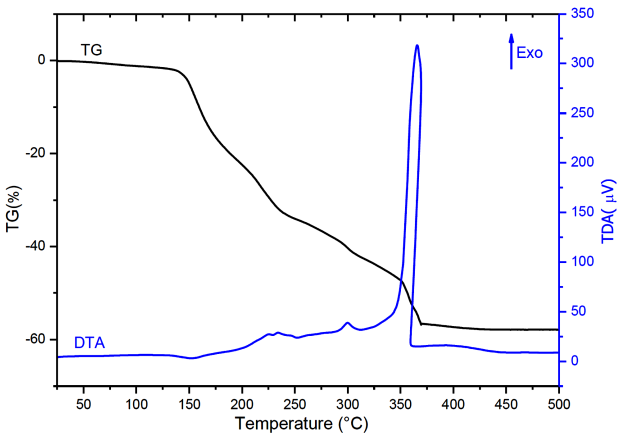

Figure 1. Simultaneous TG/DTA data measured at heating rate of 2.5 °C/min under air for $CuMo_{0.9}W_{0.1}O_4$ precursor powder

several peaks up to 370 °C. The broad endothermic peak at 150–160 °C is due to the dehydration of surface water, accompanied by weight loss in TG curve. The weak exothermic peaks between 200 and 310 °C with significant weight loss in the TG graph are assigned to the decomposition and combustion of the citrate precursor. The strong exothermic peak at 365 °C corresponds to the complete oxidation of residual carbon and the crystallization of copper molybdate, accompanied by a drastic weight loss in the TG curve.

The TG/DTA was supplemented by FTIR spectral analysis to aid further interpretation. Figure 2 shows the FTIR spectra of $CuMo_{0.9}W_{0.1}O_4$ gel heat-treated at different temperatures. IR absorption bands at different wavenumbers are marked. The FTIR spectrum of dried gel shows bands at 3420, 3225 and 3055 cm^{-1} corresponding to the H_2O and −OH groups. The band at 1720 cm^{-1} is assigned to the C=O stretching mode. Two bands at 1620 and 1404 cm^{-1} are attributed to asymmetric υ_{as}(COO) and symmetric υ_s(COO) stretching of

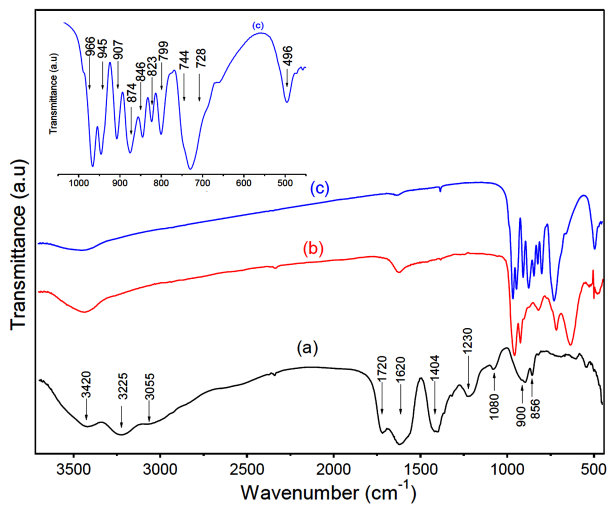

Figure 2. FTIR spectra of $CuMo_{0.9}W_{0.1}O_4$ precursor powders annealed at: a) 120, b) 300 and c) 420 °C. Insert: spectrum (c)

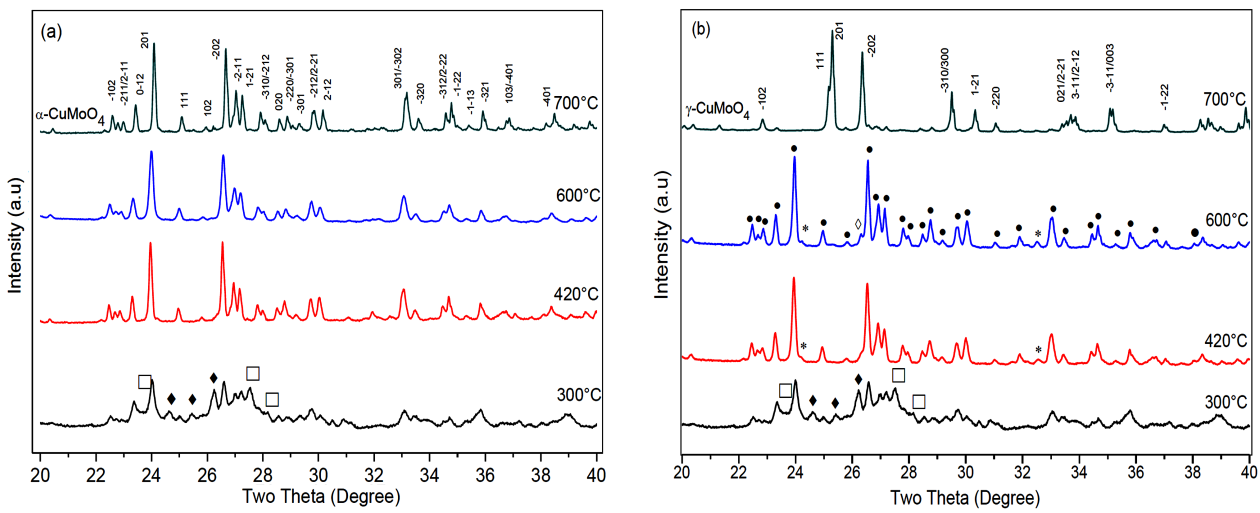

Figure 3. XRD patterns of: a) $CuMo_{0.95}W_{0.05}O_4$ and b) $CuMo_{0.9}W_{0.1}O_4$ oxides after calcination of xerogels at different temperatures (● α-$CuMoO_4$, ♦ Cu_2MoO_4, □ MoO_3, * $CuWO_4$, ◊ γ-$CuMoO_4$)

the carboxylate group, respectively [19]. The absorption bands at 1080 and 900 cm^{-1} are possibly due to δ(CO) and υ(C–C), respectively [20]. The bands at 1230 and 856 cm^{-1} are attributed to asymmetric NO_3^- stretching and bending vibrations, respectively [21]. The absorption intensity of these bands decreased with increasing temperature up to 420 °C. This indicates that the organic species have been decomposed completely at 420 °C, agreeing basically with TG/DTA analysis. The new absorption bands at 966, 945, 907, 874, 846, 823, 799, 744, 728 and 496 cm^{-1} are attributed to the vibrational mode of copper molybdate crystalline phase [22].

Figure 3 shows the crystalline phase evolution during the thermal decomposition of $CuMo_{0.95}W_{0.05}O_4$ and $CuMo_{0.9}W_{0.1}O_4$ precursors heated in air at various temperatures for 2 h. In the XRD patterns of gels calcined at 300 °C, mixtures of three phases were identified: α-$CuMoO_4$ (JCPDS 073-0488), MoO_3 (JCPDS 083-0951) and a phase that should be a mixed oxide of copper and molybdenum richer in copper than $CuMoO_4$. At 420 °C, the $CuMo_{0.95}W_{0.05}O_4$ powder was isostructural with the polymorph α-$CuMoO_4$ whereas mixtures of three phases were identified in the $CuMo_{0.9}W_{0.1}O_4$ sample: α-$CuMoO_4$, γ-$CuMoO_4$ (JCPDS 088-0620) and $CuWO_4$ (JCPDS 088-0269). After calcination at 700 °C, the $CuMo_{0.9}W_{0.1}O_4$ powder is isostructural with the polymorph γ-$CuMoO_4$ whereas in the $CuMo_{0.95}W_{0.05}O_4$, the α-$CuMoO_4$ phase persists. The polymorphic variety was dependent upon the tungsten content (Table 1). For $x \leq 0.075$, the solid solutions were isostructural with α-$CuMoO_4$ whereas for $0.075 < x \leq 0.12$ they were isostructural with the polymorph γ-$CuMoO_4$. The tungsten doping of $CuMoO_4$ stabilized the γ variety at standard conditions of pressure and temperature for tungsten contents in the range 0.075–0.120.

The microstructure of the solid solution $CuMo_{0.9}W_{0.1}O_4$ prepared by the citrate complex method was compared with that of a solid solution obtained by a conventional way according to the process described by Ehrenberg [8] (Fig. 4). The former powder was constituted of relatively spherical grains with sizes in the range 0.5–2.0 µm whereas the latter was constituted of rectangular grains with sizes larger than 10 µm. The chemical composition of the samples was checked by elemental analyses. The results are summarized in Table 1, indicating that the W/(Mo+W) ratio is in agreement with the intended stoichiometry.

3.2. *Investigation of the phase transition $\gamma \rightarrow \alpha$*

As shown on the X-ray thermo-patterns of the powder γ-$CuMo_{0.9}W_{0.1}O_4$ (Fig. 5), the γ-$CuMoO_4$ phase was sole up to 50 °C. Above this temperature, the peak 201 characteristic of the phase α-$CuMoO_4$ ($2\theta = 23.8°$) was detected. In the temperature range 50–200 °C, the intensities of the peaks of the γ-$CuMoO_4$ phase decreased at the benefit of the ones of the α-$CuMoO_4$ type

Table 1. Chemical compositions determined by energy dispersive spectroscopy (EDS) and crystalline phases detected in $CuMo_{1-x}W_xO_4$ prepared by the citrate method at 420 and 700 °C for 2 h

x	Chemical compositions	Crystalline phases detected	
	Cu : Mo : W atomic ratio	420 °C	700 °C
0.000	1.010 : 1.000 : 0.000	α-$CuMoO_4$	α-$CuMoO_4$
0.025	1.043 : 0.975 : 0.024	α-$CuMoO_4$	α-$CuMoO_4$
0.050	0.974 : 0.950 : 0.049	α-$CuMoO_4$	α-$CuMoO_4$
0.075	0.962 : 0.925 : 0.075	α, γ-$CuMoO_4$, $CuWO_4$	α, γ-$CuMoO_4$
0.100	1.028 : 0.900 : 0.102	α, γ-$CuMoO_4$, $CuWO_4$	γ-$CuMoO_4$
0.120	1.053 : 0.880 : 0.124	α, γ-$CuMoO_4$, $CuWO_4$	γ-$CuMoO_4$

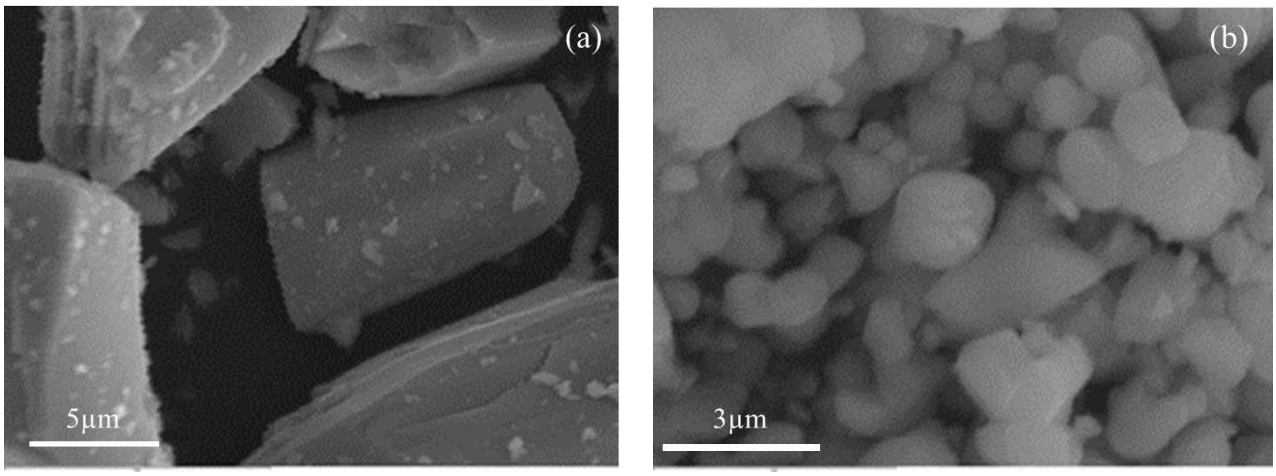

Figure 4. SEM micrographs of $CuMo_{0.9}W_{0.1}O_4$ obtained by: a) conventional method and b) citrate complex method

phase. Above 200 °C, only the α-$CuMoO_4$ phase was detectable. So, the phase transition $\gamma \rightarrow \alpha$ occurred in the temperature range 50–200 °C. The spreading of the transition temperature was attributed to the dispersion of the grain sizes of the powder, in agreement with Ponceblanc [23]. The transition temperature $T_{1/2}$, corresponding to the transformation of the half of the γ-type phase into α-type phase, was determined from the evolution of the content of the α-type phase in the $CuMo_{1-x}W_xO_4$ powders versus temperature (Fig. 6). The α-phase content (C) was calculated according to the formula:

$$C = \frac{I_\alpha}{I_\alpha + I_\gamma} 100 \quad (1)$$

where I_α and I_γ are the relative intensities of the strongest XRD peaks (201 for α and $\bar{2}02$ for γ), respectively. It can be seen that $T_{1/2}$ increases with the increase of tungsten content (Table 2). Our values are of the same order of magnitude as those measured by Yanase [1] using the differential scanning calorimetry.

The $\gamma \rightarrow \alpha$ transition occurs with a lattice volume increase of about 13% [3] which allows characterization of the transition by dilatometry. In order to specify the transition temperature, dilatometric measurements were carried out on the green pellets without any binder. For the solid solution γ-$CuMo_{0.9}W_{0.1}O_4$ (Fig. 7) a fast increase of the pellet volume, attributed to the transformation $\gamma \rightarrow \alpha$, was observed in the temperature range 95–183 °C. Then no volume change was noticed until the temperature reaches about 400 °C and above 400 °C the volume decrease was imputed to the sintering. The phase transition temperature was that for which the standardized $\Delta L/L_0 = 0.5$ [24]. The obtained values (Table 2) were in agreement with those determined by XRD in temperature. The partial isovalent substitution of molybdenum by tungsten in copper molybdate $CuMoO_4$ increased the $\gamma \rightarrow \alpha$ phase transition temperature from −23 °C for γ-$CuMoO_4$ up to 127 °C for γ-$CuMo_{0.88}W_{0.12}O_4$.

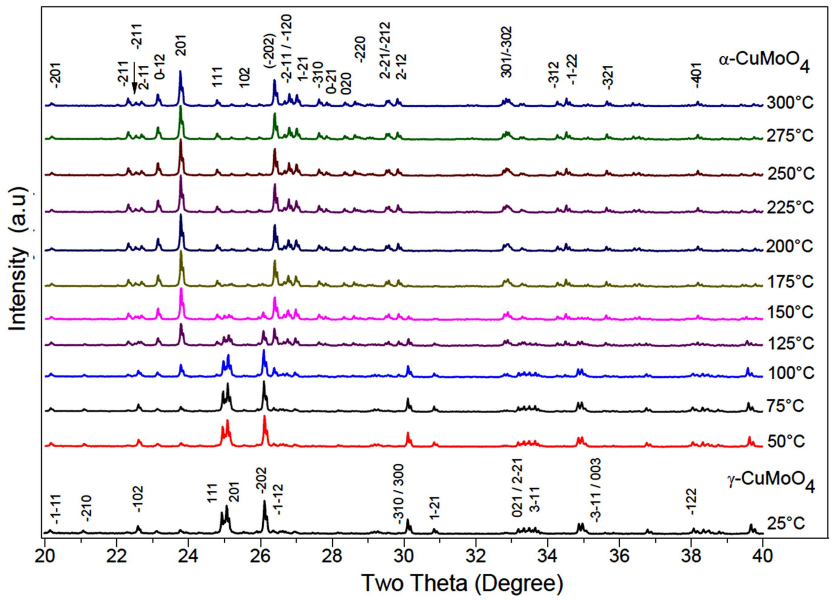

Figure 5. Influence of temperature on phase composition of γ-$CuMo_{0.9}W_{0.1}O_4$ determined by XRD

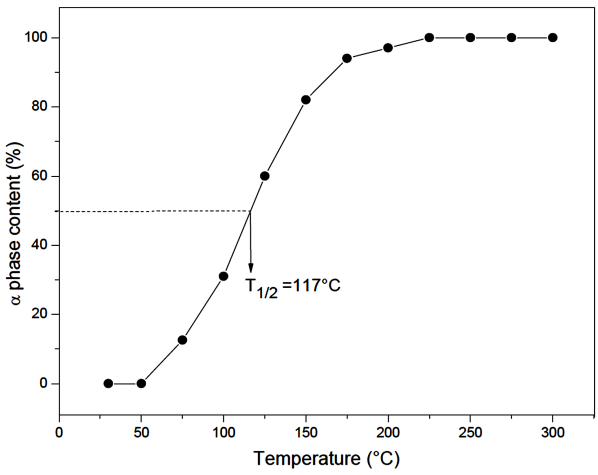

Figure 6. Influence of temperature on the α-phase content in the γ-$CuMo_{0.9}W_{0.1}O_4$ sample

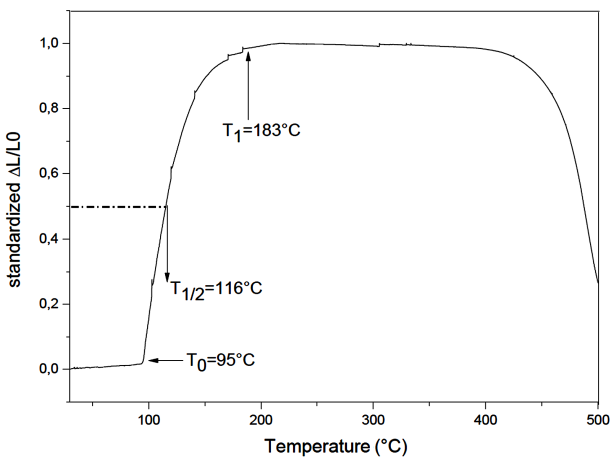

Figure 7. Normalized dilatation of γ-$CuMo_{0.9}W_{0.1}O_4$ green pellet

Table 2. $\gamma \rightarrow \alpha$ transition temperature for $CuMo_{1-x}W_xO_4$

x	X-ray diffraction	Dilatometric analysis
0.10	117	116
0.12	129	127

IV. Conclusions

Solid solutions ($CuMo_{1-x}W_xO_4$, where $0 \leq x \leq 0.12$) were obtained by pyrolysis at 700 °C for 2 hours of a precursors prepared by the citrate complex method. The XRD results revealed that the polymorphic form was dependent upon the tungsten content. For $x < 0.075$ they were isostructural with the polymorph α-$CuMoO_4$ and for $0.075 \leq x \leq 0.120$ isostructural with the polymorph γ-$CuMoO_4$. The grain size was in the range 0.5–2.0 µm. The in situ high temperature X-ray diffraction (HTXRD) and dilatometry studies revealed that the $\gamma \rightarrow \alpha$ phase transformation temperature increased with the rise of tungsten content.

Acknowledgements: This work was supported by two French-Moroccan projects: Volubilis Partenariat Hubert Curien (PHC n°: MA 09 205) and Projet de Recherches Convention Internationale du CNRS (CNRS-CNRST n°: w22572).

References

1. I. Yanase, T. Mizuno, H. Kobayashi, "Structural phase transition and thermochromic behavior of synthesized W-substituted $CuMoO_4$", *Ceram. Int.*, **39** (2013) 2059–2064.
2. G. Steiner, R. Salzer, W. Reichelt, J. Fresenius, "Temperature dependence of the optical properties of $CuMoO_4$", *J. Anal. Chem.*, **370** (2001) 731–734.
3. M. Wiesmann, H. Ehrenberg, G. Miehe, T. Peun, H. Weitzel, H. Fuess, "p-T phase diagram of $CuMoO_4$", *J. Solid State Chem.*, **132** (1997) 88–97.
4. K. Nassau, *The Physics and Chemistry of Color*, John Wiley and Sons, New York, 1983.
5. S.H. Eom, D.J. Kim, Y.M. Yu, Y.D. Choi, "Temperature-dependent absorption edge in $AgGaS_2$ compound semiconductor", *J. Alloys Compd.*, **388** (2005) 190–194.
6. J.A. Rodriguez, S. Chatuvedi, J.C. Hanson, A. Albornoz, J.L. Brito, "Electronic properties and phase transformations in $CoMoO_4$ and $NiMoO_4$: XANES and time-resolved synchrotron XRD studies", *J. Phys. Chem. B*, **102** (1998) 1347–1355.
7. A.W. Sleight, B.L. Chamberland, J.F. Weiher, "Magnetic, Moessbauer, and structural studies on three modifications of $FeMoO_4$", *Inorg. Chem.*, **7** [6] (1968) 1093–1098.
8. H. Ehrenberg, H. Weitzel, H. Paulus, M. Wiesmann, G. Wltschek, M. Geselle, H. Fuess, "Crystal structure and magnetic properties of $CuMoO_4$ at low temperature (γ-phase)", *J. Phys. Chem. Solids*, **58** (1997) 153–160.
9. P. Schmitt, N. Brem, S. Schunk, C. Feldmann, "Polyol-mediated synthesis and properties of nanoscale molybdates/tungstates: Color, luminescence, catalysis", *Adv. Funct. Mater.*, **21** [16] (2011) 3037–3046.
10. M. Benchikhi, R. El Ouatib, S. Guillemet-Fritsch, L. Er-Rakho, B. Durand, "Characterization and photoluminescence properties of ultrafine copper molybdate (α-$CuMoO_4$) powders prepared via a combustion-like process", *Int. J. Miner. Metall. Mater.*, **23** [11] (2016) 1340–1345.
11. N. Joseph, J. Varghese, T. Siponkoski, M. Teirikangas, M. Thomas Sebastian, H. Jantunen, "Glass-free $CuMoO_4$ ceramic with excellent dielectric and thermal properties for ultralow temperature cofired ceramic applications", *ACS Sustainable Chem. Eng.*, **4** [10] (2016) 5632–5639.
12. W.N. Honeyman, K.H. Wilkinson, "Growth and properties of single crystals of group I-III-VI_2 ternary semiconductors", *J. Phys. D: Appl. Phys.*, **4** [8] (1971) 1182–1185.
13. W.S. Cho, M. Yashima, M. Kakihana, A. Tudo, T. Sakata, M. Yoshimura, "Active electrochemical dissolution of molybdenum and application for room-temperature synthesis of crystallized luminescent calcium molybdate film", *J. Am. Chem. Soc.*, **80** [3] (1997) 765–770.
14. K.S. Makarevich, N.V. Lebukhova, P.G. Chigrin, N.F. Karpovich, "Catalytic properties of $CuMoO_4$ doped with Co, Ni, and Ag", *Inorg. Mater.*, **46** (2010) 1359–1364.
15. J.C. Hill, Y. Ping, G.A. Galli, K.S. Choi, "Synthesis, photoelectrochemical properties, and first principles study of n-type $CuW_{1-x}Mo_xO_4$ electrodes showing enhanced visible light absorption", *Energy Environ. Sci.*, **6** (2013) 2440–2446.
16. M. Benchikhi, R. El Ouatib, S. Guillemet-Fritsch, J.Y. Chane-Ching, L. Er-rakho, B. Durand, "Sol-gel synthe-

sis and sintering of submicronic copper molybdate (α-$CuMoO_4$) powders", *Ceram. Int.*, **40** (2014) 5371–5377.

17. M. Benchikhi, R. El Ouatib, S. Guillemet Fritsch, L. Er-Rakho, B. Durand, Kh. Kassmi, "Influence of chelating agent on the morphological properties of α-$CuMoO_4$ powder synthesized by sol-gel method", *J. Mater. Environ. Sci.*, **6** [12] (2015) 3470–3475.
18. K.T.G. Carvalho, S.C. Fidelis, O.F. Lopes, C. Ribeiro, "Effect of processing variables on the photocatalytic properties of ZnO thin films prepared using the polymeric precursor method", *Ceram. Int.*, **41** [9] (2015) 10587–10594.
19. H.S. Gopalakrishnamurthy, M. Subba Rao, T.R. Narayanan Kutty, "Thermal decomposition of titanyl oxalates - I: Barium titanyl oxalate", *J. Inorg. Nucl. Chem.*, **37** [4] (1975) 891–898.
20. J. Li, Y. Pan, F. Qiu, Y. Wu, J. Guo, "Nanostructured Nd:YAG powders via gel combustion: The influence of citrate-to-nitrate ratio", *Ceram. Int.*, **34** [1] (2008) 141–149.
21. M. Sivakumar, S. Kanagesan, K. Chinnaraj, R. Suresh Babu, S. Nithiyanantham, "Synthesis, characterization and effects of citric acid and PVA on magnetic properties of $CoFe_2O_4$", *J. Inorg. Organomet. Polym.*, **23** [2] (2013) 439–445.
22. D. Klissurski, R. Iordanova, M. Milanova, D. Radev, S. Vassilev, "Mechanochemically assisted synthesis of Cu (II) molybdate", *CR Acad. Bulg. Sci.*, **56** [8] (2003) 39–42.
23. H. Ponceblanc, J.M.M. Millet, G. Thomas, J.M. Herrmam, J.C. Védrine, "Comparative study of polymorphic phase transition by differential thermal analysis, high temperature X-ray diffraction and temperature programmed electrical conductivity measurements: case study of mixed iron and cobalt molybdate", *J. Phys. Chem.*, **96** [23] (1992) 9466–9469.
24. L.C. Robertson, M. Gaudon, S. Jobic, P. Deniard, A. Demourgues, "Investigation of the first-order phase transition in the $Co_{1-x}Mg_xMoO_4$ solid solution and discussion of the associated thermochromic behavior", *Inorg. Chem.*, **50** (2011) 2878–2884.